



# Observation of $\beta$ -delayed ${}^2\text{He}$ emission from the proton-rich nucleus ${}^{22}\text{Al}$

Y.T. Wang<sup>a,b</sup>, D.Q. Fang<sup>a,\*</sup>, K. Wang<sup>a,b,c</sup>, X.X. Xu<sup>d</sup>, L.J. Sun<sup>d</sup>, P.F. Bao<sup>d</sup>, Z. Bai<sup>e</sup>, X.G. Cao<sup>a</sup>, Z.T. Dai<sup>a</sup>, B. Ding<sup>e</sup>, W.B. He<sup>a</sup>, M.R. Huang<sup>e</sup>, S.L. Jin<sup>d</sup>, C.J. Lin<sup>a</sup>, M. Lv<sup>a</sup>, L.X. Liu<sup>a</sup>, Y. Li<sup>e</sup>, P. Ma<sup>e</sup>, J.B. Ma<sup>e</sup>, J.S. Wang<sup>e</sup>, S.T. Wang<sup>e</sup>, J.G. Wang<sup>e</sup>, H.W. Wang<sup>a</sup>, S.Q. Ye<sup>a</sup>, Y.Y. Yang<sup>e</sup>, C.L. Zhou<sup>a</sup>, M.H. Zhao<sup>e</sup>, H.Q. Zhang<sup>d</sup>, Y.G. Ma<sup>a,c</sup>, W.Q. Shen<sup>a,c</sup>

<sup>a</sup> Shanghai Institute of Applied Physics, Chinese Academy of Sciences, Shanghai 201800, China

<sup>b</sup> University of the Chinese Academy of Sciences, Beijing 100049, China

<sup>c</sup> School of Physical Science and Technology, ShanghaiTech University, Shanghai 201203, China

<sup>d</sup> China Institute of Atomic Energy, Beijing 102413, China

<sup>e</sup> Institute of Modern Physics, Chinese Academy of Sciences, Lanzhou 730000, China

## ARTICLE INFO

### Article history:

Received 29 May 2018

Accepted 17 July 2018

Available online 23 July 2018

Editor: D.F. Geesaman

## ABSTRACT

The  $\beta$ -delayed two-proton emission from  ${}^{22}\text{Al}$  was investigated experimentally through the implantation-decay method. A  $\beta$ -delayed two-proton decay branch from  ${}^{22}\text{Al}$  were identified based on the coincidence of the charged particles and  $\gamma$ -ray signals. The relative momentum ( $q_{pp}$ ) and the opening angle ( $\theta_{pp}$ ) distributions of the two  $\beta$ -delayed protons are measured and a strong peak at  $q_{pp} \sim 20$  MeV/c, as well as a peak at  $\theta_{pp} \sim 30^\circ$  are observed clearly. The  $\beta$ -delayed  ${}^2\text{He}$  emission from  ${}^{22}\text{Al}$  with a probability of 29 (13)% by fitting the experimental data with the results of Monte Carlo simulations.

© 2018 The Author(s). Published by Elsevier B.V. This is an open access article under the CC BY license (<http://creativecommons.org/licenses/by/4.0/>). Funded by SCOAP<sup>3</sup>.

## 1. Introduction

In the past few decades, researches on nuclei with extreme isospin are at the forefront of nuclear physics. Exotic phenomena including new decay modes (direct particle emission,  $\beta$ -delayed particle emission) [1,2], new structures (cluster, skin, halo structure) [3] and new magic numbers [4–6] have been found in nuclei far from the  $\beta$ -stability line. These new phenomena can help us to better understand nuclear forces and they are very important for the improvement of nuclear theoretical models. For nuclear halo structure with two valence nucleons, the existence of Cooper pairs due to the attractive pairing interaction between the two valence fermions also attracts much attention and there are also some experimental reports on this subject [7]. The momentum and angular correlations in two particle decay of proton (neutron) rich nuclei may provide an optimum chance to investigate the Bardeen–Cooper–Schrieffer (BCS) phenomena in finite nuclei [8].

The proton-rich nucleus  ${}^{22}\text{Al}$  is a  $T_z = -2$   $\beta$ -delayed two-proton emission precursor [9–11]. Fig. 1 shows a proposed partial decay scheme for  ${}^{22}\text{Al}$  [11]. A  $\beta 2p$  decay channel from the Isobaric

Analogue State (IAS) of  ${}^{22}\text{Mg}$  to the first excited state in  ${}^{20}\text{Ne}$  was confirmed by proton-gamma coincidences [11]. However, there is still no clear picture for the mechanism of this two-proton emission process. Generally speaking, there are three modes of two-proton emission:  ${}^2\text{He}$  emission, democratic three-body emission and sequential emission [12–16]. Until now, there are only one experiment performed in 1985 to measure the angular correlations between the two protons in the  $\beta$ -delayed two proton emission of  ${}^{22}\text{Al}$  [17]. In that experiment, a trace of 15%  ${}^2\text{He}$  emission was claimed in the decay process by the distribution of two-proton opening angle, but no relative momentum information was provided and the statistics was quite poor.

Nuclear reaction method is also an effective way to investigate two-proton decay mechanism. In this method, the radioactive secondary nuclei are excited in the collision process with a target. The excited nuclei may decay by two-proton emission. The correlation information between the two protons could be established. There have been several studies on  ${}^{17,18}\text{Ne}$  and  ${}^{28,29}\text{S}$  and prominent features of  ${}^2\text{He}$  cluster decay was observed in  ${}^{18}\text{Ne}$  and  ${}^{29}\text{S}$  [12, 18,19]. Recently, Ma et al. have investigated the mechanism of two-proton emission from the excited states of  ${}^{22}\text{Mg}$  through the collision of the secondary  ${}^{22}\text{Mg}$  beams with  ${}^{12}\text{C}$  target [13]. Around 30%  ${}^2\text{He}$  emission probability was observed based on the relative

\* Corresponding author.

E-mail address: dqfang@sinap.ac.cn (D.Q. Fang).

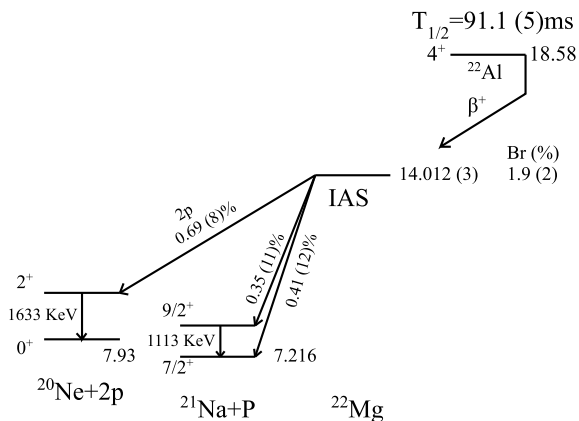


Fig. 1. Partial decay scheme of  $^{22}\text{Al}$ .

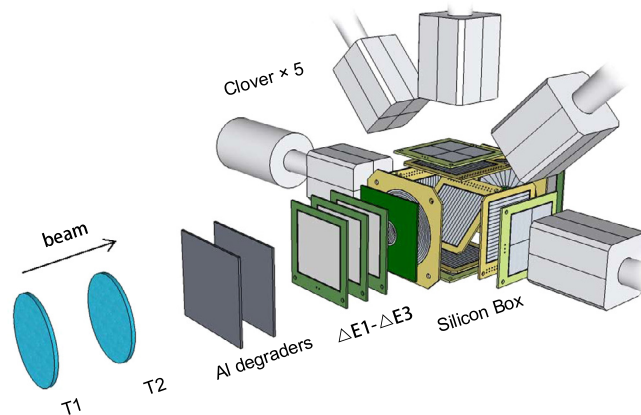


Fig. 2. The experimental setup of detectors.

momentum and opening angle distributions between the two protons emitted from  $^{22}\text{Mg}$  with a wide excitation energy window ( $12.5 < E^* < 18$  MeV). But it is difficult to determine the exact initial and final transition states in that experiment due to the wide range of the excitation energy and also missing of  $\gamma$ -rays measurement. Besides those experiments, time-projection chamber (TPC) have been used to study the rare ground state  $2p$  decay such as  $^{45}\text{Fe}$  [14] and  $^{54}\text{Zn}$  [15]. TPC method can show us a clear picture of the decay process and provide direct measurements.

In this letter, the two-proton emission mechanism was investigated by  $\beta 2p$  decay from  $^{22}\text{Al}$  with continuous implantation-decay method. Silicon array detection as well as high-purity germanium (HPGe) detectors were used in our experiment. The excited states of  $^{22}\text{Mg}$  were populated through the  $\beta$  decay of  $^{22}\text{Al}$ . Two proton decay from the IAS (14.012 MeV) in  $^{22}\text{Mg}$  to the first excited state of  $^{20}\text{Ne}$  was confirmed by the correlation between charged particles and  $\gamma$ -rays. Compared to the nuclear reaction method, the  $\beta$ -delayed two-proton decay branch could be clearly specified, and the correlation information was directly obtained event by event in the present studies. Based on the relative momentum and opening angle distributions of the two protons, a strong  $^2\text{He}$  emission component from the IAS of  $^{22}\text{Mg}$  to the first excited state of  $^{20}\text{Ne}$  was clearly observed.

## 2. Experiment description

The experimental study of the  $\beta 2p$  decay for  $^{22}\text{Al}$  was performed on the Radioactive Ion Beam Line in Lanzhou (RIBLL1) [20], China.  $^{22}\text{Al}$  was produced by the fragmentation of a  $76 \text{ A MeV } ^{28}\text{Si}$  primary beam with an average current of 50 nA on a  $384.8 \text{ mg/cm}^2$  Be target. Then the secondary beam was transported and purified through the RIBLL1. Typical intensity of  $^{22}\text{Al}$  was 0.3 pps. The main contaminants in the secondary beam were  $^{21}\text{Mg}$ ,  $^{20}\text{Na}$  and  $^{19}\text{Ne}$ .

The detection array was composed of detectors for incident ion identification and decay products detection. The identification of secondary radioactive beam was performed by means of energy loss and time-of-flight (TOF) measurements. Two scintillation detectors (at the first focal plane T1 and the second focal plane T2) and several silicon detectors ( $\Delta E$ ) were installed in the upstream of the decay position. Two measurements with almost the same secondary beams but different set-up of decay detectors were performed at RIBLL1. Continuous-implantation method was used in the two measurements. The decay detection setup of the first measurement is shown in Fig. 2 and it is described as follows. A  $16 \times 16$  double-sided silicon strip detector (DSSD)  $69 \mu\text{m}$  thick and  $5 \times 5 \text{ cm}^2$  of active area in the center of the silicon box was

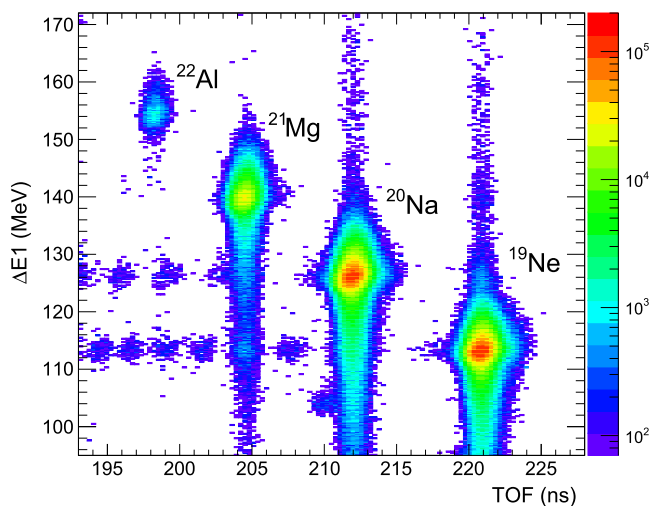
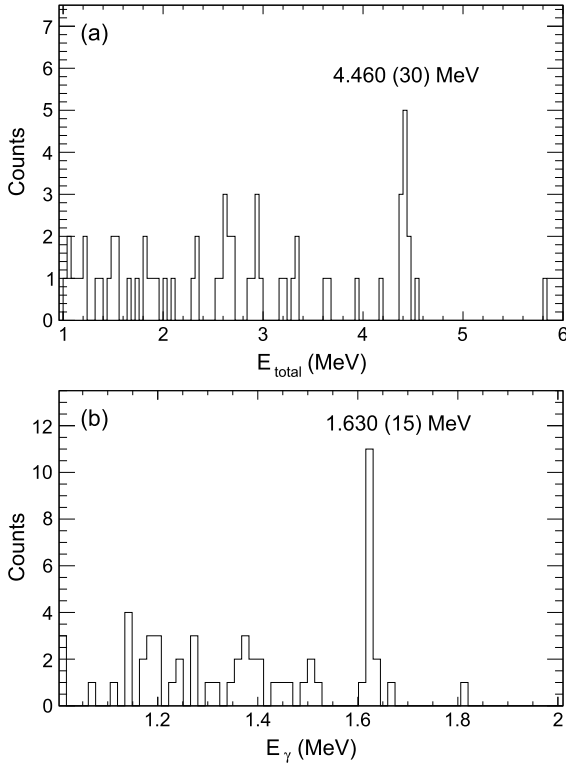


Fig. 3. Contour plot of the correlations between the energy loss in  $\Delta E1$  and TOF between T1 and T2. (For interpretation of the colors in the figure(s), the reader is referred to the web version of this article.)

served as implantation detector, and a  $42.5 (1)^\circ$  tilt angle for the implantation detector was set to get a better detection efficiency for the decay particles. Four DSSDs followed by four quadrant silicon detectors (QSDs) were located on the four side (up, bottom, left, right) of the silicon box. The thickness for the four DSSDs were  $64 \mu\text{m}$ ,  $61 \mu\text{m}$ ,  $304 \mu\text{m}$ ,  $525 \mu\text{m}$ , and for the four followed QSDs were  $1533 \mu\text{m}$ ,  $1546 \mu\text{m}$ ,  $314 \mu\text{m}$ ,  $309 \mu\text{m}$ , respectively. Two CD silicon detectors ( $317 \mu\text{m}$ ,  $315 \mu\text{m}$ ) together with other DSSDs formed a  $4\pi$  silicon box to measure the emitted charged particles which have enough energies to escape the centered  $69 \mu\text{m}$  DSSD. Angular and relative momentum correlations could also be reconstructed easily with the decay detection setup. In addition, five HPGe detectors were set in the outskirts of the silicon box to detect  $\gamma$ -rays during the measurement. Monte Carlo simulations showed that detection efficiency of the silicon box for  $^{22}\text{Al}$   $\beta 2p$  decay was about 20%. The correlation between the TOF between T1 and T2 and the energy loss in  $\Delta E1$  (TOF- $\Delta E1$ ) for the incident ions is shown in Fig. 3. The decay detection setup of the second measurement is described as follows. A  $149 \mu\text{m}$  thick DSSD was used as a implantation detector and it can detect the  $\beta$ -delayed particles at the same time.  $10 \text{ mm}$  downstream of the DSSD, another thinner  $66 \mu\text{m}$  DSSD was installed as the same function of the first DSSD but aimed for  $\beta$ -delayed protons at lower energy. Besides, the two DSSDs could also be used to detect protons escaping from the other one, so we could rebuild the angular and relative mo-



**Fig. 4.** The energy spectrum of  $\beta$ -decayed charged-particles from  $^{22}\text{Al}$  in coincidence with 1.630 (15) MeV  $\gamma$ -rays (a). The  $\gamma$  energy spectrum in coincidence with the charged-particle energy at 4.460 (30) MeV (b). The data in this figure is the summed results from the two measurements.

mentum correlations for  $\beta$ -delayed 2p. In addition, several QSDs were also installed for anti-coincidences and  $\beta$  particles detections in the experiment. Five HPGe outside the silicon detectors were used to detect the  $\gamma$ -rays emitted in the decay. A detailed description on this setup of detectors can be found in Ref. [21]. A total number of  $1.8 \times 10^5$   $^{22}\text{Al}$  were recorded in the two measurements, and a total number of 38  $\beta 2p$  events from the IAS of  $^{22}\text{Mg}$  to the first excited state of  $^{20}\text{Ne}$  were observed.

### 3. Results and discussions

When the secondary beams  $^{22}\text{Al}$  were implanted and stopped into one pixel of the implantation DSSD, the  $\beta$ -delayed particles could be detected in the same pixel of the DSSD if the implanted nuclei decayed via  $\beta$ -delayed one or two protons. If the energy of the  $\beta$ -delayed proton is high enough to escape the implantation silicon detector, it could be detected by the surrounding silicon detectors of the silicon box. The details of the continuous implantation-decay method used in our experiment could be found in Ref. [21,22]. To confirm a  $\beta 2p$  decay branch clearly, particle- $\gamma$  coincidences are needed. Fig. 4 shows the total energy spectrum of  $\beta$ -delayed charged-particles in coincidence with 1.630 (15) MeV  $\gamma$ -rays (Fig. 4 (a)) and the  $\gamma$ -rays energy spectrum in coincidence with the  $\beta$ -delayed charged-particles energy at 4.460 (30) MeV (Fig. 4 (b)) for  $^{22}\text{Al}$ . The coincidence of the  $\beta$ -delayed charged particles energy at 4.460 (30) MeV with the 1.630 (15) MeV  $\gamma$ -rays from the de-excitation process of  $^{20}\text{Ne}$  demonstrated the  $\beta 2p$  decay branch of  $^{22}\text{Al}$ , which is also confirmed by the previous experiment [11].

To obtain the distribution of relative momentum and opening angle of the two  $\beta$ -delayed protons, only those  $\beta 2p$  events with the two protons escaped the implantation DSSD and detected by the surrounding DSSDs could be selected. When the  $\beta 2p$  events

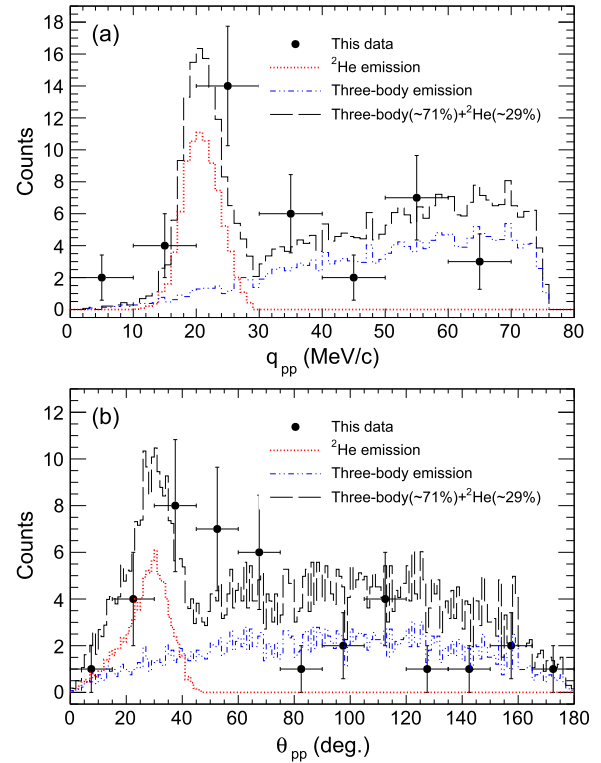


**Fig. 5.** Relative momentum (a) and opening angle (b) distributions between the two protons emitted from the IAS of  $^{22}\text{Mg}$  to the first excited state of  $^{20}\text{Ne}$ . The experimental data were shown by the solid circles. Monte Carlo simulations for the mechanism of  $^2\text{He}$  decay and three-body simultaneous emission were presented by the dash-dotted and dashed lines, respectively. The long-dashed line showed the fitted result with the experimental data, which composed of 29 (13)%  $^2\text{He}$  decay and 71 (15)% three-body simultaneous emission. The data in this figure is the summed results from the two measurements.

were confirmed, the opening angle ( $\theta_{pp}$ ) and the relative momentum ( $q_{pp} = |\mathbf{p}_1 - \mathbf{p}_2|/2$ ) can be constructed event by event according to the implantation position, the energies and stop positions of the two  $\beta$ -delayed protons in the surrounding detectors. The sum energy of the two  $\beta$ -delayed protons was around 4.460 MeV and that was measured by the implantation silicon detector and one or two surrounding silicon detectors. In our data analysis procedure, an equal energy division of the energy loss in the implantation silicon detector was assumed for the two  $\beta$ -delayed protons.

In order to investigate the mechanism of  $\beta 2p$  decay for  $^{22}\text{Al}$  to the first excited state of  $^{20}\text{Ne}$ , Monte Carlo simulations have been performed to help us to better understand the experimental results. Details on the description of the simulation method can be found in Ref. [13]. It should be noticed that in the Monte Carlo simulations, it is hard to distinguish between the two weak correlation mechanisms: sequential emissions and three-body simultaneous emissions through  $q_{pp}$  and  $\theta_{pp}$  distributions and therefore only two extreme cases, i.e.,  $^2\text{He}$  emission and three-body simultaneous emission have been considered as in Ref. [12,13].

Fig. 5 shows the experimental and simulation results of the distribution of relative momentum and opening angle for the two  $\beta$ -delayed protons from  $^{22}\text{Al}$ . We can learn from the figure that compared to the wide distributions of the relative momentum and opening angle of weak correlation three-body simultaneous emission, the  $^2\text{He}$  emission tends to have a sharp relative momentum distribution at  $q_{pp} \sim 20$  MeV/c and also a narrow opening angle distribution at small angles ( $\theta_{pp} \sim 30^\circ$ ) due to a quasi-bound  $s$ -singlet configuration. The experimental data can be interpreted by a mixed mechanism of  $^2\text{He}$  cluster decay and three-body weak

correlation decay. By fitting the experimental data with the Monte Carlo simulation results, a mixed mechanism of 29 (13)%  $^2\text{He}$  emission and 71 (15)% three-body simultaneous emission was obtained, which is very close to the experimental results by Ma et al. via the nuclear reaction method with the  $^{22}\text{Mg}$  excitation energy window of  $12.5 < E^* < 18$  MeV [13].

There is another highly possible  $\beta 2p$  decay branch to the ground state of  $^{20}\text{Ne}$ . However, it is hard to investigate the mechanism of this  $\beta 2p$  decay for low statistics and no  $\gamma$ -rays emission in this decay branch. Future experimental investigation with higher statistics and better purified secondary radioactive beams is needed to get a more accurate results.

#### 4. Conclusion

The  $\beta$ -delayed two-proton emission from  $^{22}\text{Al}$  was studied experimentally by the implantation-decay method at the RIBLL1 facility in Lanzhou, China. The excited states of  $^{22}\text{Mg}$  were populated through the  $\beta$ -decay of  $^{22}\text{Al}$ . Two-proton emissions from the IAS of  $^{22}\text{Mg}$  to the first excited state of  $^{20}\text{Ne}$  were observed based on the coincidence of the charged particle and  $\gamma$ -ray signals. The momentum and emission angle of the two protons were measured by silicon detector arrays, from which the relative momentum and opening angle distributions between the two emitted protons were obtained. A remarkable peak in the relative momentum at  $q_{pp} \sim 20$  MeV/c, as well as a peak at small opening angle were observed clearly. After fitting with the Monte Carlo simulation results, it is determined for the first time that the probability of  $^2\text{He}$  emission from the IAS of  $^{22}\text{Mg}$  to the first excited state of  $^{20}\text{Ne}$  was 29 (13)%.

#### Acknowledgements

We would like to thank the members of the RIBLL1 group and the accelerator staffs for all their support and excellent operation

of the facility in delivering the  $^{28}\text{Si}$  beam and tuning of  $^{22}\text{Al}$ . This work is partially supported by the National Key R&D Program of China under Contract No. 2018YFA0404404 and the National Natural Science Foundation of China under Contract Nos. 11421505, 11475244 and 11175231.

#### References

- [1] M.J.G. Borge, *Phys. Scr.* 2013 (2013) 014013.
- [2] M. Pfützner, *Phys. Scr.* 2013 (2013) 014014.
- [3] Ahmed N. Abdullah, *Internat. J. Modern Phys. B* 26 (2017) 1750048.
- [4] A. Ozawa, T. Kobayashi, T. Suzuki, K. Yoshida, I. Tanihata, *Phys. Rev. Lett.* 84 (2000) 5493.
- [5] O. Sorlin, M.-G. Porquet, *Prog. Part. Nucl. Phys.* 61 (2008) 602.
- [6] D. Steppenbeck, et al., *Nature* 502 (2013) 207.
- [7] T. Nakamura, et al., *Phys. Rev. Lett.* 96 (2006) 252502.
- [8] K. Hagino, H. Sagawa, J. Carbonell, P. Schuck, *Phys. Rev. Lett.* 99 (2007) 002506.
- [9] M.D. Cable, J. Honkanen, R.F. Parry, S.H. Zhou, Z.Y. Zhou, Joseph Cerny, *Phys. Rev. Lett.* 50 (1983) 404.
- [10] B. Blank, F. Boué, S. Andriamonje, R. Del Moral, J.P. Dufour, A. Fleury, P. Pourre, M.S. Pravikoff, N.A. Orr, K.-H. Schmidt, E. Hanelt, *Nuclear Phys. A* 615 (1997) 52.
- [11] N.L. Achouri, F. de Oliveira Santos, M. Lewitowicz, B. Blank, J. Aysto, G. Cachel, S. Czajkowski, P. Dendooven, A. Emsallem, J. Giovinozzo, N. Guillet, A. Jokinen, A.M. Laird, C. Longour, K. Perajarvi, N. Smirnova, M. Stanoiu, J.-C. Thomas, *Eur. Phys. J. A* 27 (2006) 287.
- [12] G. Raciti, G. Cardella, M. De Napoli, E. Rapisarda, F. Amorini, C. Sfienti, *Phys. Rev. Lett.* 100 (2008) 192503.
- [13] Y.G. Ma, et al., *Phys. Lett. B* 743 (2015) 306.
- [14] K. Miernik, et al., *Phys. Rev. Lett.* 99 (2007) 192501.
- [15] P. Ascher, et al., *Phys. Rev. Lett.* 107 (2011) 102502.
- [16] D.Q. Fang, et al., *Phys. Rev. C* 94 (2016) 044621.
- [17] R. Jahn, et al., *Phys. Rev. C* 31 (1985) 1576.
- [18] C.J. Lin, et al., *Phys. Rev. C* 80 (2009) 014310.
- [19] C.J. Lin, et al., *Nuclear Phys. A* 834 (2010) 450c.
- [20] Z.Y. Sun, W.L. Zhan, Z.Y. Guo, G.Q. Xiao, J.X. Li, *Nucl. Instrum. Methods A* 503 (2003) 496.
- [21] L.J. Sun, et al., *Nucl. Instrum. Methods A* 804 (2015) 1.
- [22] X.X. Xu, et al., *Phys. Lett. B* 766 (2017) 312.